Journal of Radiation Research, Vol. 61, No. 5, 2020, pp. 755–765
doi: 10.1093/jrr/rraa054
Advance Access Publication: 28 July 2020

Positional repeatability and variation in internal and external markers during volumetric-modulated arc therapy under end-exhalation breath-hold conditions for pancreatic cancer patients

Makoto Sasaki[1,2], Mitsuhiro Nakamura[1,3,*], Tomohiro Ono[3], Ryo Ashida[3], Michio Yoshimura[3], Manabu Nakata[2], Takashi Mizowaki[3] and Naozo Sugimoto[1]

[1]Human Health Sciences, Graduate School of Medicine, Kyoto University, Kyoto, Japan
[2]Clinical Radiology Service, Kyoto University Hospital, Kyoto, Japan
[3]Radiation Oncology and Image-applied Therapy, Graduate School of Medicine, Kyoto University, Kyoto, Japan
*Corresponding author. Human Health Sciences, Graduate School of Medicine, Kyoto University, 53 Kawahara-cho, Shogoin, Sakyo-ku, Kyoto 606-8507, Japan. Tel: +81-75-751-4176; Fax: +81-75-771-9749; Email: m_nkmr@kuhp.kyoto-u.ac.jp
(Received 13 April 2020; revised 28 May 2020; editorial decision 23 June 2020)

ABSTRACT

The purpose of this study was to assess the positional repeatability of internal and external markers among multiple breath-hold (BH) sessions and evaluate the positional variation of these markers within BH sessions for volumetric-modulated arc therapy (VMAT) for pancreatic cancer patients. A total of 13 consecutive pancreatic cancer patients with an internal marker were enrolled. Single full-arc coplanar VMAT was delivered under end-exhalation BH conditions while monitoring the internal marker with kilovoltage (kV) X-ray fluoroscopy. Positional repeatability of the internal and external markers was determined by the difference between the reference and zero position in all BH sessions, and positional variation was defined by the displacement from the reference position in each BH session during megavolt beam delivery. The overall positional repeatability was 0.6 ± 1.5 mm in the X-axis for the centroid of the internal marker (CoIM), -0.1 ± 2.2 mm in the Y-axis for the CoIM, and 0.8 ± 2.2 mm for the external marker. The frequency of an internal marker position appearing > 2 mm from the reference position in the Y-axis, despite the external marker position being ≤ 2 mm from the reference position, ranged from 0.0 to 39.9% for each patient. Meanwhile, the proportion of sessions with positional variation ≤ 2 mm was 93.2 and 98.7% for the CoIM and external marker, respectively. External marker motion can be used as a surrogate for pancreatic tumor motion during BH-VMAT delivery; however, margins of ~5 mm were required to ensure positional repeatability.

Keywords: internal marker; external marker; breath-holding; kV X-ray monitoring; pancreatic cancer

INTRODUCTION

Radiotherapy is among the treatment options for patients with locally advanced unresectable pancreatic cancer [1]. However, it is difficult to deliver a sufficient dose to the tumor because the pancreas is surrounded by radiosensitive organs at risk (OARs) of severe radiation-induced toxicity. Advanced techniques, such as intensity-modulated radiation therapy and volumetric-modulated arc therapy (VMAT), are effective in reducing the dose to the OARs while maintaining dose coverage to the tumor. Recently, VMAT is increasingly being used in clinical practice due to its ability to rapidly deliver beams [2].

Pancreatic tumors are known to move with respiration [3], which is an important consideration when treating pancreatic cancer with VMAT [4]. Respiratory organ motion can result in underdosage of the target or overdosage of surrounding OARs [5]. To address this problem, respiration motion management techniques, such as abdominal compression, breath-hold (BH), respiratory gating and real-time tumor tracking, have been used during the course of treatment [3]. Of these techniques, BH is one of the most commonly used owing to its versatility [2]. Some researchers reported that BH was clinically useful in cases with disease sites, such as the lung, breast, liver and

Table 1. Characteristics of patients treated for pancreatic cancer

ID	Sex	Age (years)	Tumor location	3D tumor motion (mm)	PTV–PRV volume (cm^3)
1	M	77	Body	11.0	225.8
2	M	85	Head	12.8	159.3
3	F	77	Head	13.0	164.8
4	F	48	Head	10.5	135.3
5	M	61	Head	20.8	220.8
6	F	86	Head	10.5	104.0
7	F	69	Head	12.0	366.9
8	F	79	Head	8.2	107.3
9	F	66	Body	11.0	119.7
10	M	64	Head	11.0	155.7
11	F	59	Head	10.9	176.2
12	F	55	Head	11.0	156.9
13	F	83	Body	10.4	145.8

M = Male; F = female.

pancreas [6–11]. At our institution, VMAT has been used clinically under BH conditions at the end-exhalation (EE) phase for pancreatic cancer [9, 12].

When applying VMAT under EE–BH conditions for pancreatic cancer patients at our institution, an infrared (IR) reflective plastic box is placed on the abdominal surface as an external marker to monitor the patient's respiratory motion. Meanwhile, a gold coil (Visicoil; IBA, Louvain-la-Neuve, Belgium) is implanted around or inside the target as an internal surrogate. However, implantation is not always acceptable to the patient due to its invasiveness. Thus, it is preferable to estimate internal motion based on the external marker without implantation.

Several investigators have assessed positional uncertainties in pancreatic cancer under BH conditions [9–12]. Nakamura *et al*. showed that the positional reproducibility of the pancreas under EE–BH conditions was 0.6 ± 3.3 mm in the superior–inferior (SI) direction, using a visual feedback technique based on daily cone-beam computed tomography (CBCT) [9]. Lens *et al*. concluded that the motion of pancreatic tumors under inhalation BH conditions was 4.2 ± 2.3 mm in the SI direction, as shown by intratumoral fiducial markers and kilovoltage (kV) X-ray fluoroscopic images [10]. Zeng *et al*. showed that the mean motion of an internal marker was -0.6 ± 2.3 mm in the SI direction, observed intermittently under inhalation BH conditions on kV X-ray images [11]. However, there have neither been any reports assessing the positions of pancreatic tumors on a continuous basis, nor about the relationship between internal and external marker motion during VMAT under EE–BH conditions.

The aim of this study was to assess the positional repeatability of internal and external markers within multiple BH sessions, as well as the positional variation of the markers within BH sessions for VMAT under EE–BH conditions for pancreatic cancer patients. The results of this study could be used to determine the suitability of external marker motion as a surrogate for pancreatic tumor motion during BHs.

MATERIALS AND METHODS

Patients

Among all pancreatic cancer patients who underwent VMAT under EE–BH conditions between July 2016 and July 2017, 13 consecutive patients with an internal marker were enrolled in this study (Table 1). As an internal marker, a Visicoil (10-mm long and 0.5 or 0.75-mm in diameter) was endoscopically inserted into the tumor 1 to 2 weeks before treatment-planning computed tomography (CT). More than 8 mm of 3D internal marker motion was visually confirmed by a radiation oncologist using kV X-ray fluoroscopy under free breathing just before the treatment-planning CT scan. All patients fasted for > 3 h and oral intake of water was stopped 1 h before the treatment-planning CT scan and daily treatments. This study was performed in accordance with the Helsinki Declaration and was approved by our institutional review board (approval number: R1446).

CT scans and organ delineation

All patients were immobilized by individualized vacuum pillows (Bofy Fix; Elekta, Stockholm, Sweden) in supine position with their arms raised. The breathing signal was acquired using an IR marker block attached to the abdominal surface of the patient and the Real-time Position Management System (RPM; Varian Medical Systems, Palo Alto, CA, USA) with a sample frequency of 30 Hz. In accordance with our institutional BH protocols, patients held their breath according to only the operator's coaching, without visual feedback; an operator instructed the patients to 'breathe in and breathe out' while monitoring their breath signals using the RPM systems and to 'hold their breath' at the end-exhalation. After several BH trainings, two planning CT scans with/without contrast enhancement were performed under EE–BH conditions with a 16-slice CT scanner (LightSpeed RT16; GE Healthcare, Little Chalfont, UK). The CT scan range was from the superior border of the liver to the iliac crest, which took ~15 s, and then the CT datasets were imported to the radiation treatment planning system (Eclipse version 13.7.14; Varian Medical Systems).

The gross tumor volume, clinical target volume (CTV) and OARs, including the stomach, duodenum, intestine, liver, kidneys and spinal cord, were manually delineated on the CT images without contrast enhancement. The planning target volume (PTV) was determined by adding a 5 mm isotropic margin to the CTV. The planning OAR volume (PRV) was generated by adding ~3–5 mm of isotropic

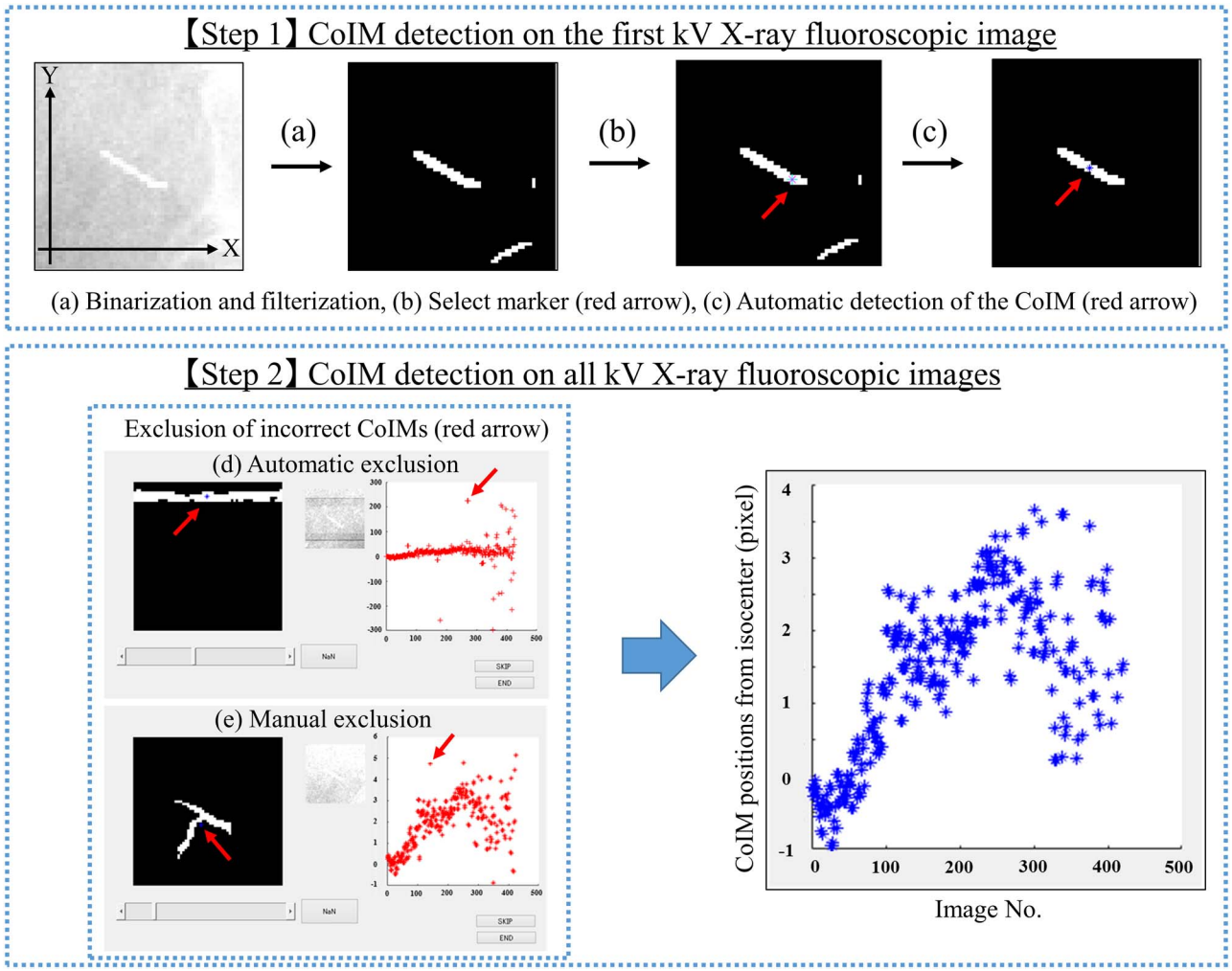

Fig. 1. Procedure for detecting the centroid of the internal marker (CoIM). In Step 1, the CoIM is detected on the first kilovoltage (kV) X-ray fluoroscopic image. The fluoroscopic image was binarized and had a Hessian-based multiscale filter applied (a). Manual selection of the internal marker (b) and automatic detection of the CoIM (c). In Step 2, the algorithm automatically detected the CoIM on all kV X-ray fluoroscopic images. Thereafter, images with incorrect CoIMs were excluded automatically (d) and manually (e).

margin to the stomach, duodenum and spinal cord. More detailed planning CT scan protocols and organ delineation have been provided previously [9, 12, 13].

Treatment planning

The single full-arc coplanar VMAT plan (gantry angle, 181–179° in the clockwise direction) was created with the TrueBeam STx system (Varian Medical Systems) for all patients. The nominal energy and maximum dose rate were 10-MV flattening filter-free photon beams and 2400 monitor units (MU)/min, respectively. A dose of 48 Gy in 15 fractions was prescribed in order to cover 95% of the PTV, subtracting the overlapping part of the PRVs. The planned isocenter was set to the center of the internal marker. The dose–volume constraints have been shown previously [14].

Daily treatment procedure

First, initial setup errors were corrected by referring to bony structures using an orthogonal kV X-ray imaging system (ExacTrac X-ray system, version 6.2.1; Brainlab, Feldkirchen, Germany). Subsequently, CBCT images were acquired in 2 or 3 BHs, each ~20 s, by interrupting the acquisition once or twice depending on the patient's BH ability. The BH protocols for CBCT acquisition were performed similarly to the planning CT scan. The final isocenter position was determined by correcting setup errors based on the internal marker positions in the planning CT and CBCT images. Thereafter, the center position of the internal marker was monitored on kV X-ray fluoroscopic images (pixel size: 0.368 mm at the isocenter, sample frequency: 25 Hz), acquired in the left–right (LR) direction (kV X-ray beam direction of 91°) for a few seconds under EE–BH conditions using the kV X-ray imager. Unless the internal marker position was within 2 mm of the planned isocenter,

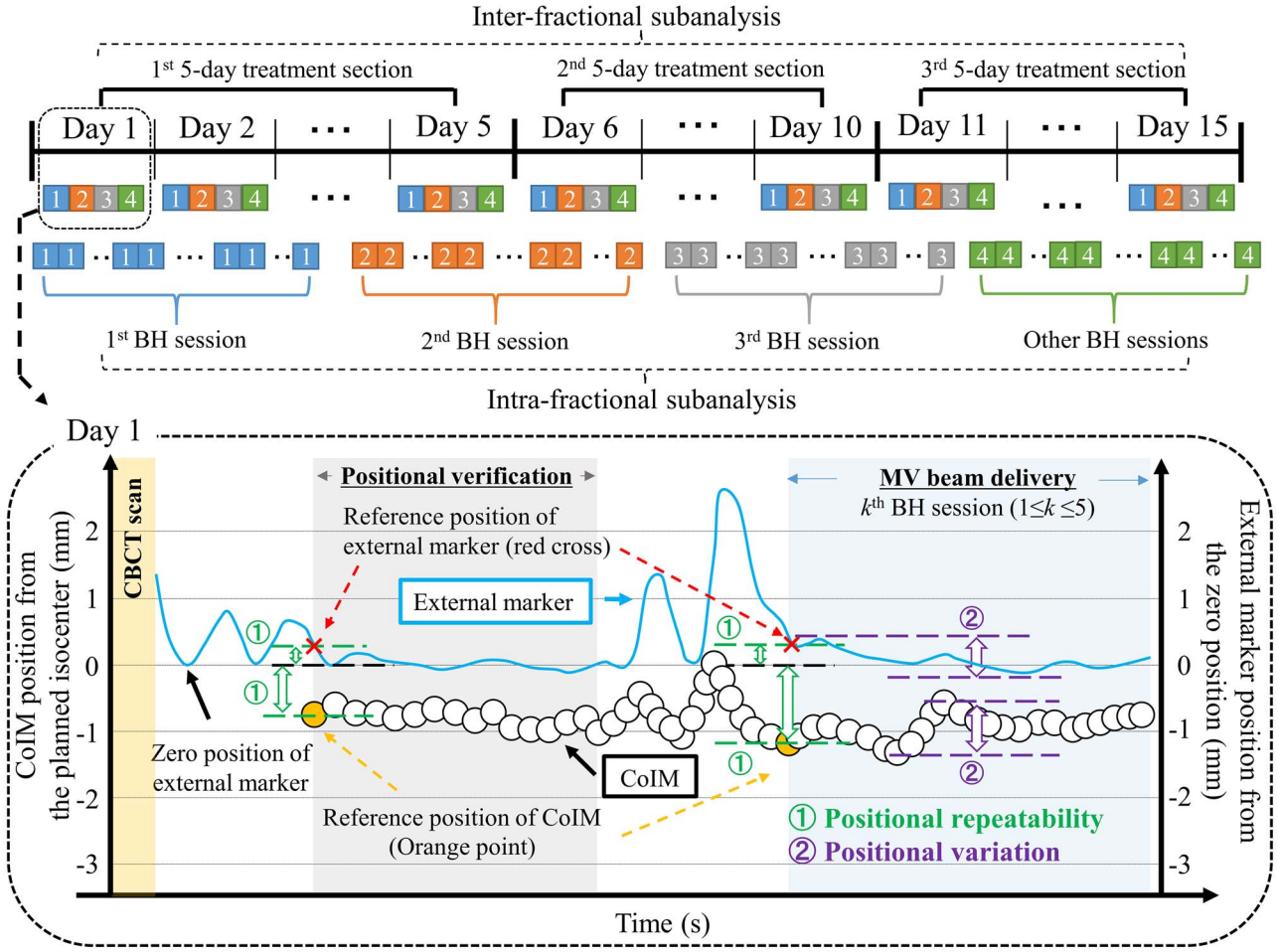

Fig. 2. Positional uncertainties of the centroid of the internal marker and external marker. The zero position of the external marker was defined as the most posterior position in the first respiratory cycle in the Real-time Position Management signals under free breathing, reacquired after cone-beam computed tomography.

BH was repeated several times while monitoring the kV X-ray fluoroscopic images to confirm the internal marker position. If the internal marker position was still >2 mm from the planned isocenter, CBCT images were reacquired under EE–BH conditions. This procedure was repeated until the internal marker position was within 2 mm of the planned isocenter on the kV X-ray fluoroscopic images under EE–BH conditions. This process is referred to as 'positional verification'.

After confirming that the internal marker position was within 2 mm from the planned isocenter, single full-arc coplanar VMAT was delivered under EE–BH conditions while monitoring the internal marker using kV X-ray fluoroscopy with a tube current of up to 7 mA. The 10-MV beam was delivered over 2–5 BH sessions (each ~15–30 s, depending on the patient's BH ability) for a single arc. When the center of the internal marker visually exceeded 2 mm from the planned isocenter on kV X-ray fluoroscopy for ~3 s, the beam was manually turned off. If the internal marker was again within 2 mm of the planned isocenter, the beam was manually turned on. This process is referred to as 'MV beam delivery'. Simultaneously, the IR marker block on the abdominal surface of the patient was monitored using the RPM (Varian Medical Systems).

Image processing

The centroid of the internal marker (CoIM) was detected on the kV X-ray fluoroscopic images and acquired during BH using in-house software programmed using MATLAB (version 2017b; MathWorks, Natick, MA, USA).

Figure 1 illustrates the procedure used for CoIM detection. First, all kV X-ray fluoroscopic images were binarized to emphasize the internal marker, and a Hessian-based multiscale filter was applied to enhance the internal marker (Fig. 1a). A Hessian-based multiscale filter emphasizes elongated or tubular structures by combining a Hessian matrix with Gaussian convolution to tune the filtering response to the specific scales [15]. Second, the internal marker position on the first kV X-ray fluoroscopic image after BH was determined manually, and the CoIM was calculated automatically on all kV X-ray fluoroscopic images (Fig. 1 b and c). Thereafter, detected positions that exceeded three times the median absolute deviation were automatically excluded as incorrect CoIMs (Fig. 1d). Finally, we visually verified whether the CoIM had been correctly detected on all images. If the position was found to be erroneous, the image was manually excluded from the analyses (Fig. 1e). Here, the Y-axis indicated the SI direction on the kV X-ray

Table 2. Positional repeatability among breath-hold (BH) sessions and positional variation within BH sessions for all patients[a]

	Positional repeatability between BHs (mm)							Positional variation during BH (mm)			
	CoIM				External marker		CoIM >2 mm in the Y-axis, and external marker ≤2 mm	CoIM		External marker	
	X-axis		Y-axis		AP			Y-axis		AP	
Patient	Mean	SD	Mean	SD	Mean	SD	Ratio (%)	Mean	SD	Mean	SD
1	0.5	0.9	0.6	0.9	−0.1	1.7	5.5	0.5	0.4	0.3	0.3
2	0.3	1.2	−1.1	2.2	2.0	2.3	15.5	0.9	0.7	0.8	0.7
3	0.6	1.6	−0.2	2.6	2.7	2.1	16.1	0.6	0.4	0.3	0.3
4	0.6	1.4	0.3	1.8	−0.5	1.0	15.6	0.7	0.6	0.3	0.3
5	0.6	1.2	1.2	2.1	1.1	2.1	10.0	-	-	-	-
6	0.7	1.8	−0.5	2.0	1.4	2.0	16.4	0.8	0.7	0.6	0.5
7	0.5	0.9	0.1	0.8	1.8	1.6	0.0	0.4	0.4	0.4	0.4
8	0.7	1.7	0.4	2.4	0.6	1.0	39.0	1.1	0.9	0.4	0.4
9	0.5	1.5	−0.8	2.6	3.3	2.6	20.0	0.6	0.5	0.4	0.4
10	0.4	1.4	0.6	1.8	−0.7	1.0	18.9	-	-	-	-
11	0.7	1.0	−0.9	1.4	0.4	0.8	24.2	-	-	-	-
12	0.8	1.3	1.4	1.8	−1.4	1.7	15.5	0.9	0.8	0.4	0.4
13	1.1	1.8	1.7	2.3	0.1	1.3	39.3	0.9	0.8	0.6	0.8
All	0.6	1.5	−0.1	2.2	0.8	2.2	19.1	0.8	0.7	0.5	0.5

[a]The Y-axis indicated the superior–inferior direction on kV fluoroscopic images; the X-axis was perpendicular to the Y-axis. The positive direction in the Y-axis always corresponded to the inferior direction for patients. Note that the AP and left-right directions were composited in the X-axis depending on the gantry angle. Patients 5, 10 and 11 were excluded from the analysis of positional variation due to the extreme difficulty of CoIM detection.

fluoroscopic images; the X-axis was perpendicular to the Y-axis. The positive direction on the Y-axis corresponded to the inferior direction for patients. Note that the anterior–posterior (AP) and LR directions were composited on the X-axis depending on the gantry angle. Meanwhile, the positions of the external marker on the abdominal surface of the patient were recorded using the RPM system; signals were linearly extracted at 25 Hz to correspond to the kV X-ray fluoroscopic images.

Positional uncertainties

Figure 2 shows the definitions of positional uncertainties of the CoIM and external markers. Positional repeatability was determined by the difference between the reference and zero positions in positional verification and each BH session. The reference position of the CoIM was represented as the position from zero which was equivalent to the planned isocenter. The reference position of the external marker was represented as a position from zero which was defined as the most posterior position in the first respiratory cycle of the RPM signals under free breathing reacquired after the CBCT scan.

Positional variation was defined as the absolute displacement from the reference marker position during each BH session under MV beam delivery.

Data analysis

The means and standard deviations (SDs) of the CoIM for positional repeatability were calculated for each patient in the X- and Y-axis of the fluoroscopic images, and those of the external marker motion were calculated in the AP direction. Similarly, the means and SDs of the CoIM for positional variation were calculated for each patient in the Y-axis of fluoroscopic images, and those of the external marker motion were calculated in the AP direction. In addition, population-based margins to ensure the impact of the SD of the positional repeatability, defined as the 95th percentile of unassigned values in each axis for the internal marker, were assessed.

In this study, intra- and inter-fractional subanalyses were also conducted. Three or more BH sessions were commonly required on a treatment day. For intra-fractional subanalyses, each treatment day was divided into four sessions: 1st BH session, 2nd BH session, 3rd BH session and other BH sessions. Positional repeatability and variation were then assessed for each individual BH session. In addition, the treatment course was divided into three 5-day treatment sections to see how many differences occurred between three sections. Positional repeatability and variation were then assessed by section; details are shown in Fig. 2. One-way analysis of variance (ANOVA) was performed to evaluate differences in positional repeatability and positional variation, by BH session and by 5-day treatment section. Tukey's multiple comparison test was performed when ANOVA showed significant differences. P-values < 0.05 indicated a significant difference in both tests.

Pearson's correlation coefficients (r) between the CoIM motions in the Y-axis and the external marker motions in the AP direction during each BH session were calculated. In this study, these relationships were evaluated based on the following categorization: weak correlation, absolute correlation coefficient $|r| < 0.4$; moderate correlation, $0.4 \leq |r| < 0.7$; and strong correlation, $|r| \geq 0.7$. A regression coefficient (a) was also calculated. When the regression coefficient was > 1, the internal marker displacement was larger than the external marker displacement. Based on these datasets, the relationship between the CoIM and the external marker positions was assessed to determine whether external marker motion could be used as a surrogate for internal marker motion during BHs. In this study, a threshold of external marker motion was set to ± 2 mm from the reference position as well as that of internal marker motion.

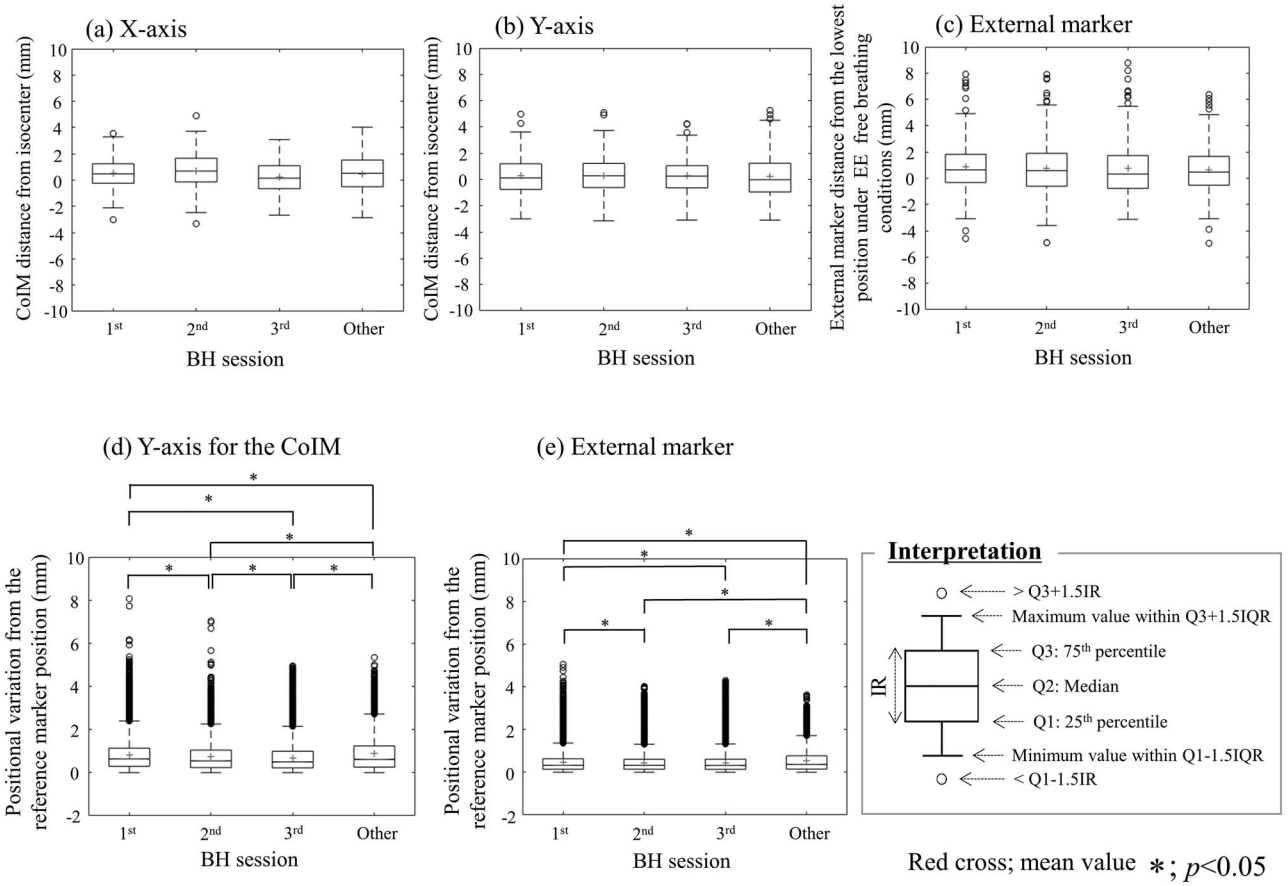

Fig. 3. Box-and-whisker plots of the intra-fractional subanalyses of positional repeatability among multiple breath-hold (BH) sessions and positional variation within BH sessions. The positional repeatability among BH sessions for the centroid of the internal marker (CoIM) on the X-axis (a) and on the Y-axis (b) and for the external marker (c). The positional variation within BH sessions for the CoIM on the Y-axis (d) and for the external marker (e). The superior–inferior direction for patients on fluoroscopic images corresponded to the Y-axis; the X-axis was perpendicular to the Y-axis.

RESULTS

Marker detection

Data from a total of 1235 BH sessions from 13 patients were obtained, including both positional verification and MV beam delivery, during the overall treatment course. In addition, the first kV X-ray fluoroscopic image of each BH session was used in the analysis of positional repeatability.

Based on the analysis of positional variation, three patients (patients 5, 10 and 11) were excluded from analysis due to extreme difficulty in detecting the CoIMs. Consequently, 697 BH sessions (10 patients) under MV beam delivery were used to analyse positional variation, encompassing a total of 260 015 datasets, all consisting of kV X-ray fluoroscopic images and the corresponding external marker positions. Ultimately, the CoIM was detected on 157 754 kV X-ray fluoroscopic images (60.7%), with some of the data being excluded due to low image contrast according to the gantry angle.

Positional repeatability and variation throughout the treatment course

Table 2 shows the positional repeatability and variation for the CoIM and external marker. The overall positional repeatability was 0.6 ± 1.5, -0.1 ± 2.2 and 0.8 ± 2.2 mm, in the X-axis for the CoIM, Y-axis for the CoIM and AP direction for the external marker, respectively. The population-based margins for positional repeatability were 3.0 and 4.6 mm in the X-axis and Y-axis, respectively. The frequency of an internal marker position appearing >2 mm from the reference position in the Y-axis, despite the external marker position being ≤2 mm from the reference position, ranged from 0.0 to 39.9% for each patient. In total, 19.1% of the 1235 BH sessions showed positional repeatability >2 mm in the Y-axis for the CoIM and ≤2 mm for the external marker.

The overall positional variation was 0.8 ± 0.7 mm in the Y-axis for the CoIMand 0.5 ± 0.5 mm in the AP direction for the external marker. The proportions of absolute positional variation ≤2 mm was 93.2 and 98.7% for the CoIM and external marker, respectively. Moreover, 93.8% of the internal marker displacement was within ±2 mm from the reference position when the external marker displacement was ≤2 mm from the reference position.

Intra- and inter-fractional subanalyses of positional repeatability and positional variation

In the intra-fractional subanalyses, there was no significant difference in positional repeatability between the 1st BH session group and the

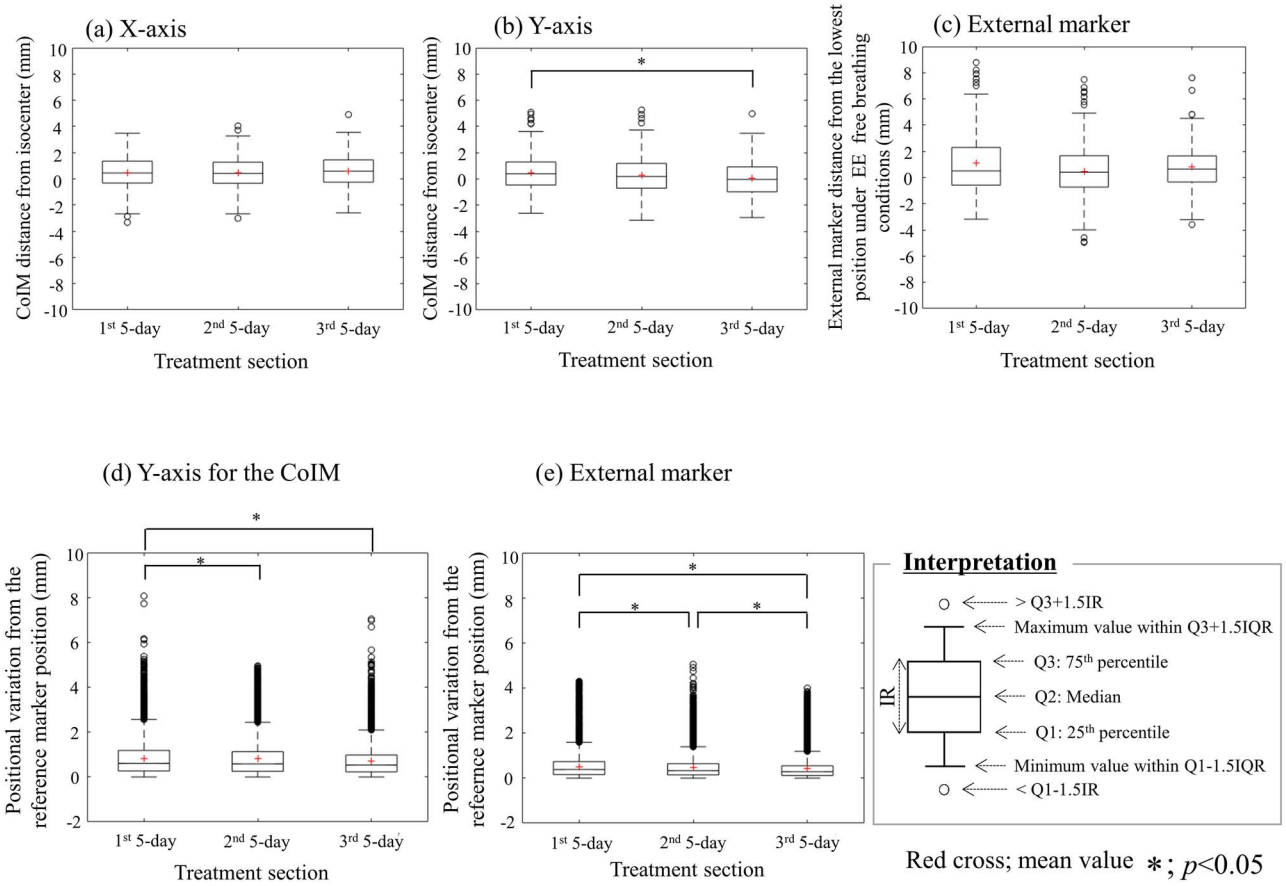

Fig. 4. Box-and-whisker plots of the inter-fractional subanalyses of positional repeatability among multiple breath-hold (BH) sessions and positional variation within BH sessions. The positional repeatability among multiple BH sessions for the centroid of the internal marker (CoIM) on the X-axis (a) and on the Y-axis (b) and for the external marker (c). The positional variation within BH sessions for the CoIM on the Y-axis (d) and for the external marker (e). The superior-inferior direction for patients on fluoroscopic images corresponded to the Y-axis; the X-axis was perpendicular to the Y-axis.

other groups, for both CoIM and external markers, during the course of treatment (Fig. 3a–c). Meanwhile, ANOVA showed significant differences in positional variation within BH sessions ($P < 0.05$), and Tukey's multiple comparison test showed significant group differences for the CoIM in the Y-axis and external marker, with the exception of the comparison between the 2nd and 3rd BH sessions for the external marker (Fig. 3d and e). The mean positional variation for the CoIM was 0.81 mm [95% confidence interval (CI) 0.80–0.82] in the 1st BH session, 0.74 mm (95% CI, 0.73–0.75) in the 2nd BH session, 0.69 mm (95% CI, 0.68–0.70) in the 3rd BH session and 0.88 mm (95% CI, 0.87–0.89) for the other BH sessions. Positional variation decreased gradually from the 1st to the 3rd BH session; however, variation increased again in the group with >3 BH sessions (Fig. 3d).

In the inter-fractional subanalyses, ANOVA showed significant differences in positional repeatability ($P < 0.05$) in the Y-axis for the CoIM and positional variation ($P < 0.05$) of both the internal and external markers. ANOVA showed no significant differences in positional repeatability in the X-axis for the CoIM or the external marker (Fig. 4a and c). Meanwhile, Tukey's multiple comparison test showed significant differences in positional repeatability in the Y-axis for the CoIM between the 1st 5-day treatment section [mean, 0.48 mm (95% CI, 0.30 to 0.67)] and the 3rd 5-day treatment section [mean, 0.05 mm (95% CI, −0.12 to 0.22)] ($P < 0.05$) (Fig. 4b). Additionally, there was a significant difference in positional variation between the 1st 5-day treatment section and the other sections ($P < 0.05$); however, no significant difference between the 2nd and 3rd 5-day treatment sections was observed in the Y-axis for the CoIM (Fig. 4 d). The mean positional variation was 0.81 mm (95% CI, 0.80 to 0.82) in the 1st 5-day treatment section, 0.80 mm (95% CI, 0.79 to 0.81) in the 2nd 5-day treatment section and 0.71 mm (95% CI, 0.70 to 0.72) in the 3rd 5-day treatment section.

Correlation between the internal and external markers

In all the BH sessions, the correlation between the CoIM and external marker positions showed a weak relationship in 54%, moderate relationship in 30% and strong relationship in 16% of the sessions (Fig. 5a). For BH sessions with weak correlation, the percentage of positional

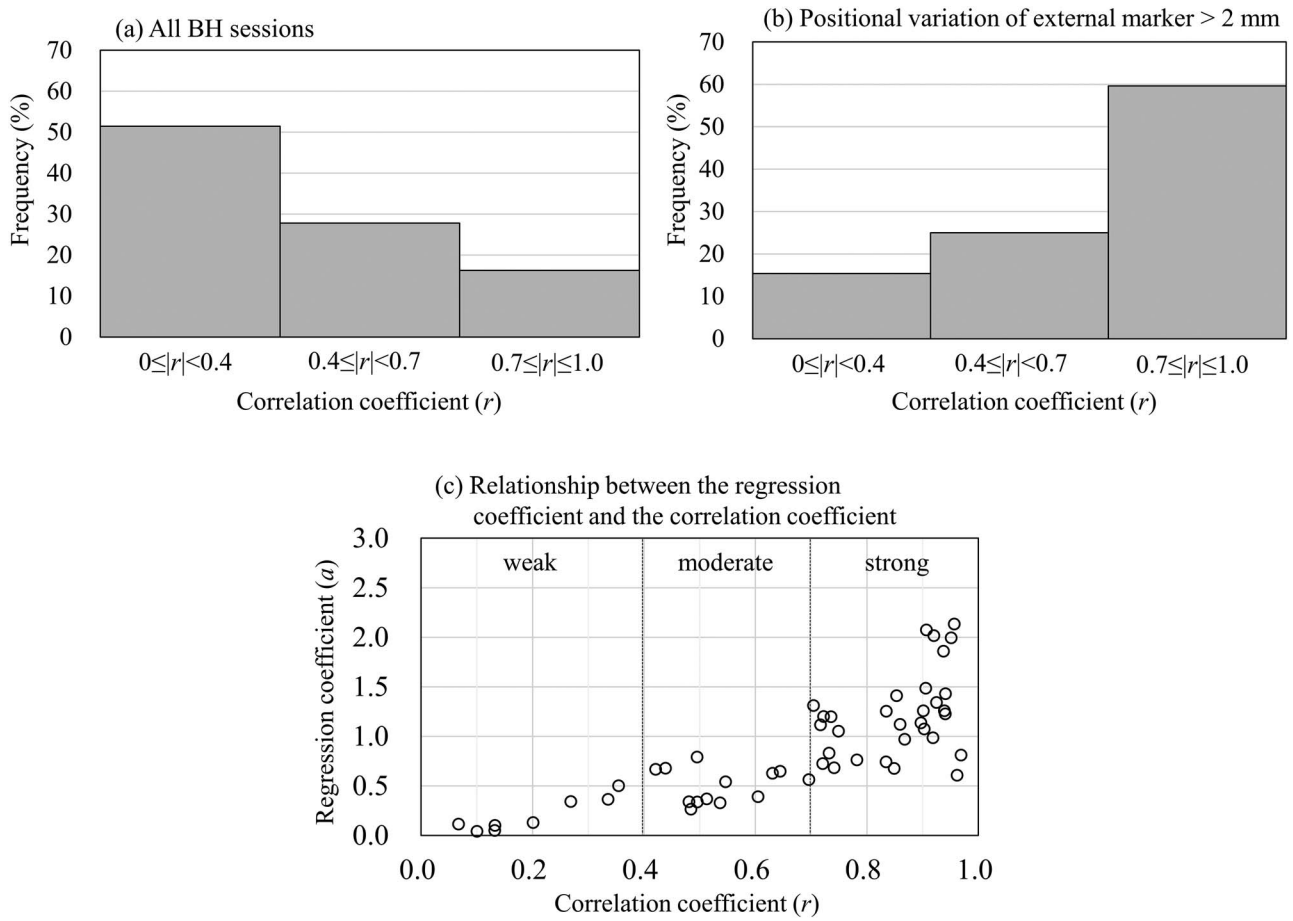

Fig. 5. Correlation between the internal and external markers. The histogram of the correlation coefficients for all breath-hold (BH) sessions (a), and that of the sessions where the positional variation of the external marker relative to the reference position after BH was >2 mm (b). The relationship between the regression coefficient (a) and correlation coefficients (r) in cases where the positional variation of the external marker exceeded 2 mm (c).

variations where both markers were within 2 mm was 96.1%. Meanwhile, 60% of BH sessions where positional variation of the external marker was $> \pm 2$ mm from the reference position showed a strong correlation between the CoIM and external marker positions (Fig. 5b). Moreover, 70% of BH sessions in which external marker motion was $> \pm 2$ mm and where there was a strong correlation between the CoIM and external marker positions had a regression coefficient >1 (Fig. 5c). Figure 6a and b show an example case (patient 8) with a weak correlation between the internal and external marker motions within BH sessions, due to a slow drift in the external marker position. Figure 6c and d show another example case (patient 4) in which there was a strong correlation between the internal and external marker motions within BH sessions, which was due to the sudden motion of both markers in the positive direction 6 s after the BH phase.

DISCUSSION

We assessed the internal and external marker motions during VMAT under EE–BH conditions for pancreatic cancer patients. In the present study, the overall positional repeatability for the CoIM was 0.6 ± 1.5 and -0.1 ± 2.2 mm in the X- and Y-axis, respectively, which was comparable with the results by Lens *et al.* [10]. We demonstrated that the CoIM often deviated from the reference position by more than 2 mm in the Y-axis, despite the external marker position being $\leq$2 mm. Based on these results, it is difficult to estimate positional repeatability of the tumor only by referencing the position of the external marker during each BH session; therefore, margins of around 5 mm are required to ensure positional repeatability, which was comparable with the results by Nakamura *et al.* [12].

Regarding positional variation, we found that both the internal and external markers drifted, even during BH (Fig. 6a and c). According to Takao *et al.*, this could be mainly due to physiological movements, such as pulsations and muscle relaxation, or an incomplete BH [16]. Meanwhile, the correlation between the internal and external marker motions during BH was weak in the majority (51%) of cases (Fig. 5a), which may represent physiological movements. Of these BH sessions, most of the positional variations of both markers were within 2 mm. From these results, we confirmed that most of the internal marker

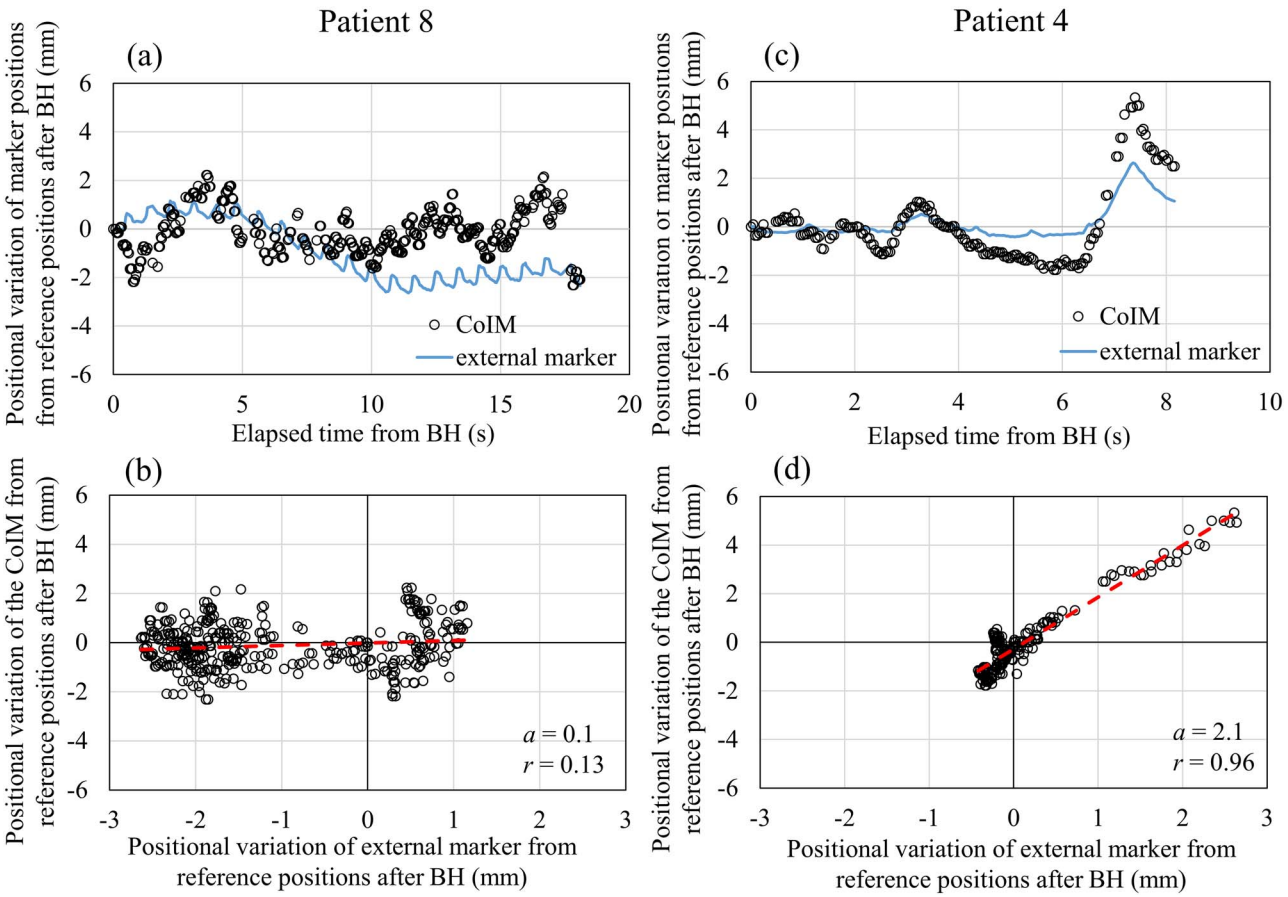

Fig. 6. A case (patient 8) showing a weak correlation between the two marker motions (a, b), and a case (patient 4) showing a strong correlation between the two marker motions (c, d). A regression line is shown in a red broken line.

displacement can be ensured to be within 2 mm as long as one monitors that the external marker displacement is <2 mm, even in a BH session with a weak correlation. In contrast, 60% of BH sessions where external marker displacement exceeded 2 mm from the reference position showed a strong correlation between the internal and external marker motions (Fig. 5b). This could represent an incomplete BH as a transition to the inhalation phase due to limits of the BH. In BH sessions with a strong correlation between the internal and external markers, monitoring the external marker motions during the BH could predict pancreatic tumor motion, as reported by Shen *et al.* [17]; therefore, we are convinced that external marker motion can generally be used as a surrogate for internal marker motion during BH despite the correlation coefficient.

In the intra-fractional subanalyses, the positional variation gradually decreased from the 1st to 3rd BH session, while the variation increased in the group with >3 BH sessions (Fig. 3d and e). In the inter-fraction subanalyses, positional variation improved during the 3rd 5-day treatment section (day 11–15), compared to that during the 1st 5-day treatment section (day 1–5). According to Lee *et al.*, BH training before treatment improved the positional consistency of lung tumors [18]. To further improve the positional consistency of pancreatic cancer motion during the 1st BH session within the first few days after beginning treatment, sufficient BH training of the patient would be useful.

Our study had several limitations. First, positional variation was analysed only in the SI direction because the magnitudes of motion in the AP and LR directions were unclear due to the dependence on the gantry angle. Whitfield *et al.* reported that inter- and intra-fractional pancreatic cancer motion was larger in the SI direction than in other directions under free breathing conditions [19], and Lens *et al.* reported that pancreatic cancer motion under inhalation–BH conditions was greater in the SI direction than in the AP direction [10]; therefore, we assume that positional repeatability and variation would be smaller in the AP and LR directions than in the SI direction. Second, we evaluated only 13 consecutive patients, and 3 patients were excluded from the positional variation analysis. The main reason was that it was impossible to continuously detect the internal marker due to strong artifacts, such as overlaps with the internal marker, dark bands and halation (Fig. 7). However, even with this small number of cases, the rough relationship between internal and external marker motion during VMAT under EE–BH conditions could be determined.

CONCLUSIONS

We found that external marker motion can generally be used as a surrogate for pancreatic tumor motion during BH; however, the internal marker position often deviated from the reference position by >2 mm in the Y-axis, even when the external marker position was within 2 mm

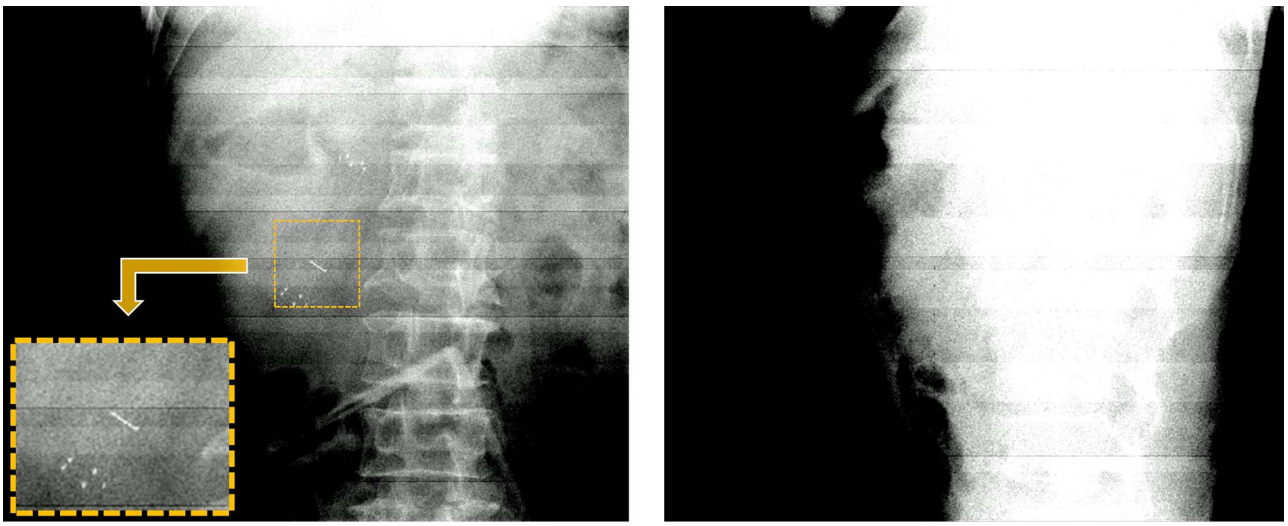

(a) Overlapping the internal marker and dark bands

(b) Halation

Fig. 7. Example of image artifacts. Overlap with the internal marker and dark bands (a), and halation (b).

of the reference position. In addition, we found that positional variation of the internal marker during BH was larger for BHs within the first few days of treatment.

FUNDING

This research was supported in part by JSPS KAKENHI (Grant Nos 18H02766, 18 K15545, 20 K16757).

CONFLICT OF INTEREST

None declared.

REFERENCES

1. Tempero MA, Malafa MP, Al-Hawary M et al. Pancreatic adenocarcinoma, version 2.2017, NCCN clinical practice guidelines in oncology. *J Natl Compr Canc Netw* 2017;15:1028–61.
2. Akino Y, Tohyama N, Akita K et al. Modalities and techniques used for stereotactic radiotherapy, intensity-modulated radiotherapy, and image-guided radiotherapy: A 2018 survey by the Japan Society of Medical Physics. *Phys Med* 2019;64:182–7.
3. Keall P, Mageras G, Balter J et al. The management of respiratory motion in radiation oncology report of AAPM task group 76. *Med Phys* 2006;33:3874–900.
4. Akimoto M, Nakamura M, Nakamura A et al. Inter- and intrafractional variation in the 3-dimensional positions of pancreatic tumor due to respiration under real-time monitoring. *Int J Radiat Oncol Biol Phys* 2017;98:1204–11.
5. Sasaki M, Nakamura M, Mukumoto N et al. Variation in accumulated dose of volumetric-modulated arc therapy for pancreatic cancer due to different beam starting phase. *J Appl Clin Med Phys* 2019;20:118–26.
6. Lu L, Diaconu C, Djemil T et al. Intra- and inter-fractional liver and lung tumor motions treated with SBRT under active breathing control. *J Appl Clin Med Phys* 2015;19:39–45.
7. Osman S, Hol S, Poortmans P et al. Volumetric modulated arc therapy and breath-hold in image-guided locoregional left-sided breast irradiation. *Radiother Oncol* 2014;112:17–22.
8. Lin Y, Ozawa S, Miura H et al. Split-VMAT technique to control the expiratory breath-hold time in liver stereotactic body radiation therapy. *Phys Med* 2017;40:17–23.
9. Nakamura M, Akimoto M, Ono T et al. Interfraction positional variation in pancreatic tumor using daily breath-hold cone-beam computed tomography with visual feedback. *J Appl Clin Med Phys* 2015;16:108–16.
10. Lens E, van der Horst A, Versteijne E et al. Considerable pancreatic tumor motion during breath-holding. *Acta Oncol* 2016;55:1360–8.
11. Zeng C, Xiong W, Li X et al. Intrafraction tumor motion during deep inspiration breath hold pancreatic cancer treatment. *J Appl Clin Med Phys* 2019;20:37–43.
12. Nakamura M, Shibuya K, Shiinoki T et al. Positional reproducibility of pancreatic tumors under end-exhalation breath-hold conditions using a visual feedback technique. *Int J Radiat Oncol Biol Phys* 2011;79:1565–71.
13. Goto Y, Nakamura A, Ashida R et al. Clinical evaluation of intensity-modulated radiotherapy for locally advanced pancreatic cancer. *Radiat Oncol* 2018;13:1–9.
14. Ziegler M, Nakamura M, Hirashima H et al. Accumulation of the delivered treatment dose in volumetric modulated arc therapy with breath-hold for pancreatic cancer patients based on daily cone beam computed tomography images with limited field-of-view. *Med Phys* 2019;46:2969–77.
15. Frangi A, Niessen W, Vincken K et al. Multiscale vessel enhancement filtering. In: Wells WM, Colchester A, Delp S (eds).

Medical Image Computing and Computer-Assisted Intervention – MICCAI 1998. Lecture Notes in Computer Science, Vol. 1496. Berlin: Springer, 1998, 130–7.

16. Takao S, Miyamoto N, Matsuura T et al. Intrafractional baseline shift or drift of lung tumor motion during gated radiation therapy with a real-time tumor-tracking system. *Int J Radiat Oncol Biol Phys* 2016;94:172–80.
17. Shen Z, Andrews M, Balik S et al. Real-time position management (RPM) system as a valuable tool to predict tumor position deviation in SBRT lung and liver patients with breath hold using active breathing coordinator (ABC). *Med Phys* 2016; 43:3440.
18. Lee D, Greer P, Lapuz C et al. Audiovisual biofeedback guided breath-hold improves lung tumor position reproducibility and volume consistency. *Adv Radiat Oncol* 2017;2:354–62.
19. Whitfield G, Jain P, Green M et al. Quantifying motion for pancreatic radiotherapy margin calculation. *Radiother Oncol* 2012;103:360–6.